AIChE

Spatially Resolved Characteristics of Pharmaceutical Sprays

Ariel R. Muliadi and Paul E. Sojka
Maurice J. Zucrow Laboratories, School of Mechanical Engineering, Purdue University, IN 47907

DOI 10.1002/aic.12775
Published online November 17, 2011 in Wiley Online Library (wileyonlinelibrary.com).

Spatially resolved drop size, velocity, and volume flux data for five different spray coating guns were described in this study. Such spatially resolved measurements show how sprays respond to changes in operating conditions and gun design in ways that less complete measurements can not provide. Data for instance, allow us to recognize the unique drop size distribution of one of the sprays tested, which ultimately was an important factor in determining the dual roles of the shaping air flows: depending on drop size, viscosity, and the magnitude of the shaping air velocity, the shaping air can either pinch or induce secondary atomization to the sprays. When the former outweighs the latter, a dumbbell-shaped spray develops; a more uniform spray results when the opposite occurs. Volume flux data from the different sprays also suggest that a more robust and consistent tablet coating process can likely be designed by utilizing multiple overlapping round sprays. © 2011 American Institute of Chemical Engineers *AIChE J,* 58: 2920–2935, 2012
Keywords: spray tablet coating, spray pattern, phase Doppler analyzer, pharmaceutical, multiphase flow

Introduction

Most pharmaceutical tablets have a thin (10–20 μm) film coating on their surface. The coating is often of significant importance as it may mask taste, improve tablet mechanical properties, separate reacting ingredients within the tablet, ease swallowing, seal the tablet from moisture to improve shelf-life, and control drug release rate and location within the patient (enteric coating).

A film coat is usually applied by subjecting tablets to an atomizer-produced spray while tumbling them inside a rotating cylindrical drum. Current implementation of this process, however, is such that film finish defects (e.g., cracks/splits in films, film peeling off tablet surfaces, poor film-to-tablet adhesion, etc.) and inter/intratablet coating nonuniformities often occur.

Finish defects are the result of several factors. Tablet-to-tablet and tablet-to-drum surface attrition are the most obvious explanations. Not often explored are the roles that the spray and its characteristics play on film coat quality. Studies that do relate film coat quality to spray characteristics are:

- Kim et al.[1] and Rowe and Forse,[2] who reported that incidences of logo infilling (bridging) increased as liquid supply rate increased.
- Twitchell,[3] Twitchell et al.,[4] and Reiland and Eber,[5] who found that increasing the atomizing air pressure or decreasing the gun-to-target distance resulted in a smoother film coat.
- Twitchell,[3] who noted that a decrease in gun-to-target distance decreased film surface roughness.
- Ruotsalainen et al.,[6] who determined that film surface roughness increased with an increase in liquid supply rate.
- Fisher and Rowe[7] and Rowe,[8] who observed that film-to-tablet adhesion decreased as liquid viscosity increased.
- Twitchell[3] and Rowe and Forse,[9] who found that increasing the local spray mass flux at the tablet bed, achieved by increasing the liquid supply rate or changing the spray pattern from elliptical to circular, decreased the incidence of film splitting.

In addition to finish defects, spray characteristics can also contribute to inter/intratablet coating nonuniformities. Relevant literature includes that by:

- Twitchell et al.,[10] Ruotsalainen et al.,[6,11] and Tobiska et al.,[12] all of whom confirmed that increasing atomizing air pressure decreased intratablet film thickness variations.
- Rege et al.[13] and Porter et al.,[14] who noted that a greater intertablet film thickness variation resulted when atomizing air pressure,[13,14] liquid viscosity, or liquid supply rate was increased.[14]

While finish defects may reduce only the aesthetic appearance of the tablets, inter/intratablet coating nonuniformities pose a more serious problem; measurements show that film thickness varied, on average, by as much as 57% from one tablet to another.[15] This is significant, especially when the film coat controls the release rate and/or release location (enteric coating) of the active ingredient(s). In such cases, the drug may be released too early—which happens when a portion of the film coat is too thin, is cracked/split, or when it is missing altogether—or too late, which happens when the film coat is too thick.

The behavior described earlier can also be explained by droplet wetting characteristics,[3,16] and by understanding how mechanical stresses are developed in film coatings.[2,16,17] Coating nonuniformities, on the other hand, likely arise from nonuniformities in sprays.[15] Accordingly, spray data that

Correspondence concerning this article should be addressed to P. E. Sojka at sojka@purdue.edu.

show how spatial distributions of spray volume flux, drop size, and drop velocity vary with changes in spraying conditions and spray gun design are important, not only because they provide comprehensive understanding on the sprays formation and evolution mechanisms, but also because they can be used as inputs to a computational fluid dynamics (CFD) model describing the tablet coating process.

Most currently available spray data, however, provide only qualitative assessment of spray uniformity. For instance, Rege et al.[13] and Porter et al.[14] speculated that spray nonuniformities were exacerbated when the atomizing air pressure was increased. No quantitative measurements were reported in either case. Studies that do provide quantitative measurements of spray characteristics (i.e., size, velocity, flux, and patternation) are limited to measurements along the spray semi-minor or semimajor axis,[3,18] or as planar-averaged data for use as inputs to CFD models.[19] Furthermore, little quantitative data are available as to how spray nonuniformities vary with other commonly used spray control parameters (liquid supply rate, shaping air pressure, gun-to-target distance, and liquid viscosity) and gun design. The immediate consequence of such poor data availability is that key control parameters and gun design features that influence spray uniformity are not unambiguously identified, and their effects on spray characteristics are not well understood (substandard process understanding). As a result, process guidelines derived from available data will most likely fail to optimize intertablet coating uniformities (substandard quality-by-design).

To address what previous efforts lack, this study presents comprehensive spray data consisting of spatially resolved spray drop size, velocity, and volume flux and their variations with common spray parameters. Emphasis is placed on the identification and understanding of key process variables and/or gun design features that appreciably affect spray uniformity and characteristics. Applications to spray modeling are also briefly discussed.

Methods

Spatially resolved mean drop size, velocity, and flux measurements were made using a dual-mode PDA system (Dantec Dynamics GmbH, Denmark). The dual-PDA was used because its combination of "standard" and "planar" photodetector pairs makes it less susceptible to slit and Gaussian beam (trajectory) effects that lead to sizing errors.[20–22] Consequently, the dual-PDA gives more accurate measure of volume flux when compared to standard PDA systems.[23]

The dual-PDA volume flux results, however, are not without limitations. Many studies have confirmed that dual-PDA volume flux data exhibit significant discrepancies when compared to experimentally measured volume flow rates. Such discrepancies arise from the following systematic limitations.

First, the dual-PDA is incapable of processing signals when multiple drops are simultaneously present in the measurement volume.[23,24] This is because, unlike number density-based (ensemble) instruments, the PDA processes each drop individually. A consequence of this feature is that the instrument sampling rate becomes limited to the nominal speed of the processing unit (typically 6 μs for modern PDA systems[23]). Anything that arrives in the measurement volume during the processor dead time (i.e., when detection algorithms are already processing a signal from a droplet) is ignored.

Several findings[20,21,25] also suggest that as drop size approaches the width of the viewing slit, the reference area with which volume flux is calculated becomes size-dependent and is no longer well-defined by the slit aperture. However, since the processing algorithms still calculate fluxes based on the dimensions of the slit-truncated measurement volume, errors in mass flux measurements can result.

Another source of error in PDA volume flux estimations is "burst-splitting."[26–29] Burst splitting occurs when interference fringes disappear and reappear while a droplet is still inside the measurement volume. This can arise when one or more drops blocks one of the laser beams. As a result, the interrogated droplet will seemingly emit two distinct burst signals. If both signals exceed the detection validation threshold, the detection algorithm will mistakenly count a single droplet twice, ultimately causing overestimation of spray volume flux.

With the exception of the processor sampling rate (dead time), all of the above volume flux-related errors can be improved by adjusting certain user-specified dual-PDA settings. Adjusting such settings, however, has proved challenging for two reasons.

First, the instrument dynamic size range[30–33] is sensitive to these settings. For instance, incorrectly setting the user-adjustable PDA signal amplification factors has been found to result in neglect of small droplets (when the PMT voltage and/or signal gain are too low), as well as photomultiplier saturation by large droplets (when PMT voltage and/or signal gain are too high).[30,31]

Second, no concrete guidelines for "optimizing" PDA measurements currently exist. For unclear reasons, PDA studies are most often performed by either maximizing the data rate or by compromising between maximum data rate and maximum validation rate. Neither was chosen in this investigation. Instead, instrument parameters were set such that PDA-measured mass (volume) flux matched independently measured mass flux supplied to the atomizer (this matching process will be referred to as "mass closure" in subsequent discussions). This decision was made on the basis that accurate spray mass (volume) information is of significant importance when optimizing intertablet coating uniformities.

Mass (volume) closure was achieved in the following manner. The total spray volume flow rate entering an atomizer was measured using a MicroMotion FO25S Coriolis flow meter. The dual-PDA was then used to acquire spatially resolved drop size, velocity and volume flux data on a 2.5 $\times$ 2.5 mm grid for round sprays, and on a 5 $\times$ 5 mm grid for elliptical sprays. Total volume flow rate was then determined by multiplying all local volume flux values by their corresponding grid areas.

Subsequent spatially resolved drop size, velocity and volume flux measurement sets were acquired after iteratively adjusting LDA/PDA and optical PDA instrument settings until the PDA-calculated and MicroMotion-measured volume flow rates were within 10% of each other. Agreement was usually achieved by adjusting the validation threshold-related quantities to restrictive levels and keeping signal amplification low. This was done primarily to reduce noise in the burst signals. Doing so also reduces the Gaussian beam and slit sizing errors, since such a validation scheme automatically filters out signals with small amplitude that typically correspond to those resulting from a nondominating scattering order.[20,34] Typical values of PMT voltage, signal gain,

Table 1. LDA/PDA Selections for the Dual-PDA

PDA Parameters	Values
PMT voltage	700–800 V
Signal gain	0
Burst detector SNR	2–5 dB
Level validation ratio	2–8
(Fixed) record length	32–64

burst detector SNR, and level validation ratio are provided in Table 1.

In addition to the settings listed, the width of the burst signal was truncated to a fixed length that corresponded to approximately half the width of the burst signal at the most dense location in the spray. This was done by setting the record length to "fixed" and specifying it to be 32 or 64. Doing this further reduces signal noise, and may prevent over-counting of drops due to burst-splitting events by shortening the interrogation interval.

Typical Optical PDA settings for the dual-PDA are summarized in Table 2. The use of manufacturer-supplied aperture Mask C, combined with receiver and transmitter focal lengths of, respectively, 310 and 160 mm, ensured detection of droplets as large as 100 μm and, after accounting for the 50:1 dynamic range,[23] as small as 2 μm. Such a range envelops the size distribution of typical air-assist sprays, and is therefore suitable for this study.

Table 2 shows that the spherical validation band was set to 30%. This value was chosen to ensure that the maximum number of large (and most likely to distort) drops were recognized. The aperture slit width was chosen to be as narrow as possible to ensure uniform illumination of the measurement volume, yet wider than the diameter of the largest drop to prevent errors in flux measurements due to inaccurate reference area estimation.[20] Since droplet diameters were generally smaller than 80 μm, all experiments were performed using the 100 μm slit. A total of 150,000 samples were collected at each measurement point, except at the spray peripheries where there were fewer drops than at the spray center. At these locations, collecting 150,000 samples was impractical; therefore samples were instead collected over a period of 120 seconds, during which approximately 25,000 to 45,000 samples were typically collected. Finally, signal processing was conducted using BSA-Flow Software v4.00 (Dantec Dynamics GmbH, Denmark). No "offline" correction to the flux measurements, such as those described in Roisman et al.,[24] was used.

It is important to note that dual-PDA measurements performed using the above settings give data that are quantitatively similar to those obtained from an extinction tomography-based optical patternator (OP-600, En'Urga).[35]

Atomizers

Spatially resolved data were acquired from sprays produced by a total of five atomizers. They are categorized as:

Table 2. Optical PDA Parameter Selections for the Dual-PDA

PDA Properties	Values
Aperture mask	C
Spherical validation band	30%
Spatial filter	Slit width: 100 μm

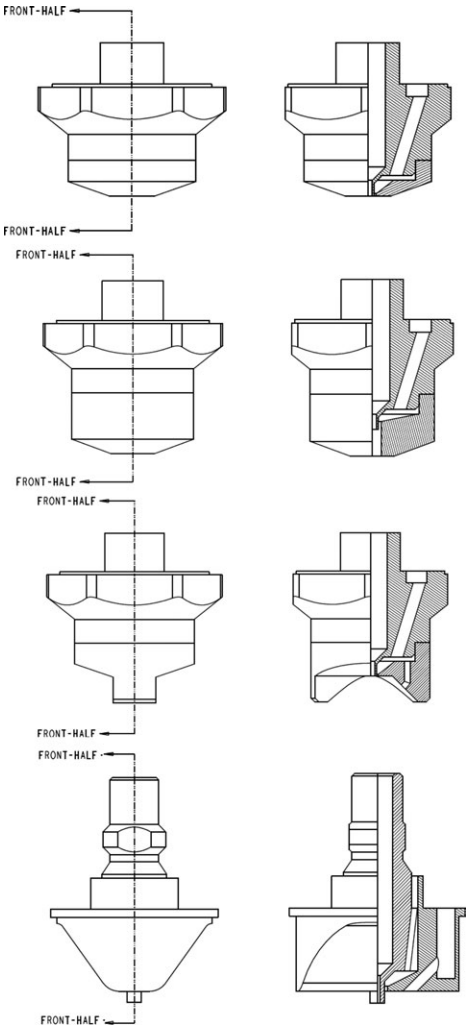

Figure 1. Cross-sectional view of the various cap designs.

From top are Atomizers D, E, C, and A. Atomizer B shares a similar design to Atomizer A.

- Those having an elliptical spray pattern:
  - Two external-mix, air-assist types with flat-shaped air caps: Schlick 930/7-1-S35 and Schlick 970/0-S-75 (Dusen-Schlick GmbH, Germany). The former gun—referred to as atomizer "A" hereafter—employs a spring loaded antidrip mechanism. It is designed for use with higher liquid supply rates and is three times as large as the latter gun (atomizer "B"). Both atomizers A and B feature antibearding liquid caps.
  - An external-mix, air-assist type with a 45° horn-shaped conventional cap (atomizer "C"): Spraying Systems 1/4-JAU-SS-SUE15B-SS (Spraying Systems Co., USA).
- Those having a circular spray pattern:
  - An external-mix, air-assist type: Spraying Systems 1/4-JAU-SS-SU1-SS (atomizer "D").
  - An internal-mix, air-assist type: Spraying Systems 1/4-JAU-SS-SU11-SS (atomizer "E").

Cross-sectional views of the different atomizers appear as Figure 1. Atomizer operational parameters are listed in Table 3. Unless otherwise noted, water was the sprayed liquid.

It is important to note that the elliptical sprays used in this study are similar to the ones produced by Twitchell et al.[36] and Mueller and Kleinebudde.[37] They are also

Table 3. Atomizer Operational Conditions

Condition	Atomizer	p_{AA}^{+} (kPa)	p_{SA}^{++}(kPa)	$\dot{m}_{liq}^{+++}$(g/min)	Gun-to-Target Distance (cm)	Data Shown in
1a	A	205	140	80	14	Figure 2a
2a	A	275	140	80	14	Figure 2b
3a	A	275	210	80	14	Figure 2c
4a	A	275	140	110	14	Figure 2d
5a	A	275	140	110	16.5	Figure 2e
1b	B	140	140	80	14	Figure 3a
2b	B	205	140	80	14	Figure 3b
3b	B	205	205	80	14	Figure 3c
4b	B	140	140	110	14	Figure 3d
5b	B	140	140	110	16.5	Figure 3e
1c	C	345	–	100	12.5	Figure 4a
2c	C	450	–	100	12.5	Figure 4b
3c	C	345	–	100	10	Figure 4c
4c	C	345	–	130	10	Figure 4d
1d	D	345	–	100	10	Figure 5a
2d	D	450	–	100	10	Figure 5b
3d	D	450	–	130	10	Figure 5c
4d	D	450	–	130	12.5	Figure 5d
1e	E	345	–	60 (205 kPa)	10	Figure 8a
2e	E	345	–	85 (275 kPa)	10	Figure 8b
3e	E	345	–	110 (345 kPa)	10	Figure 8c
4e	E	345	–	110 (345 kPa)	12.5	Figure 8d

+ atomizing air pressure.
++ shaping air pressure.
+++ liquid supply rate.

commonly found in industrial- and lab-scaled drum coaters. The round sprays are presented as benchmarks for the elliptical sprays. Furthermore, atomizers A and B feature separately controlled shaping and atomizing air inlets. This allows the shaping air flows to be completely shut off, thereby producing sprays with a circular pattern.

Results

Influence of gun design on spray characteristics

The size, velocity, and volume flux distributions of the five sprays are presented as contour plots in Figures 2–6 for atomizers A to E, respectively. These figures not only

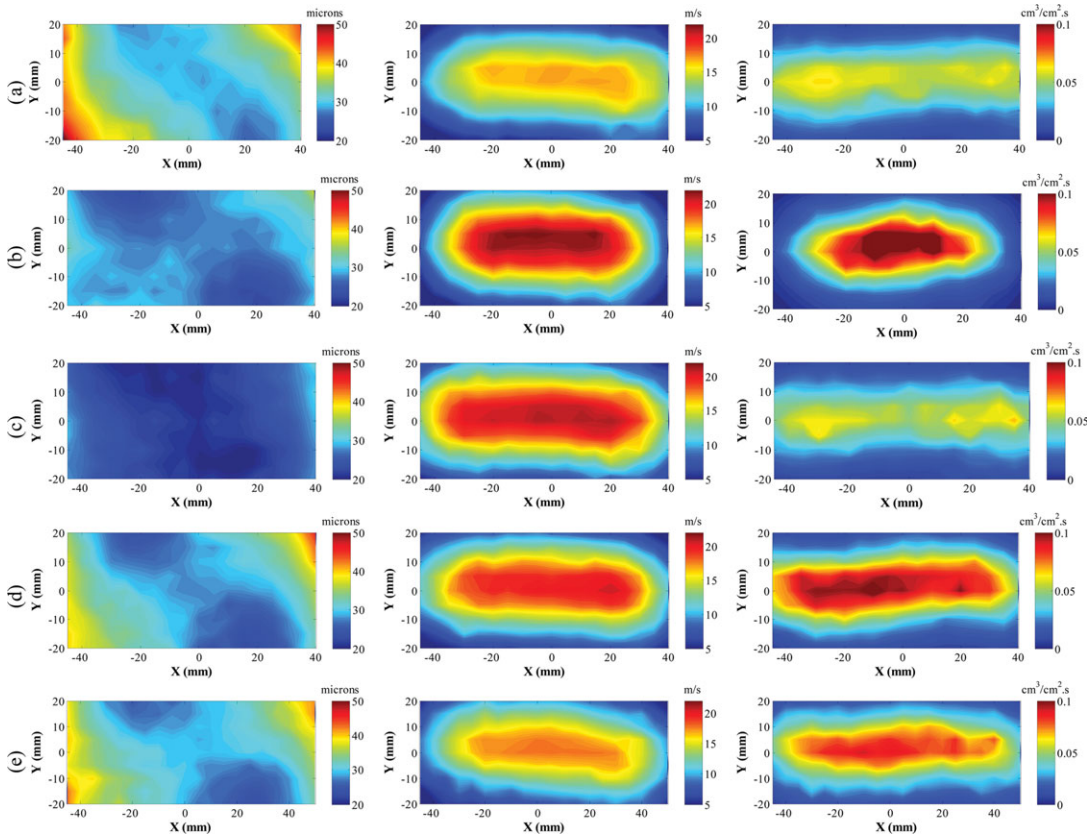

Figure 2. Diameter (D_{32}) (left), velocity (middle), and volume flux (right) data for Atomizer A sprays.

(a)–(e) show data for spraying conditions 1a–5a, respectively. [Color figure can be viewed in the online issue, which is available at wileyonlinelibrary.com.]

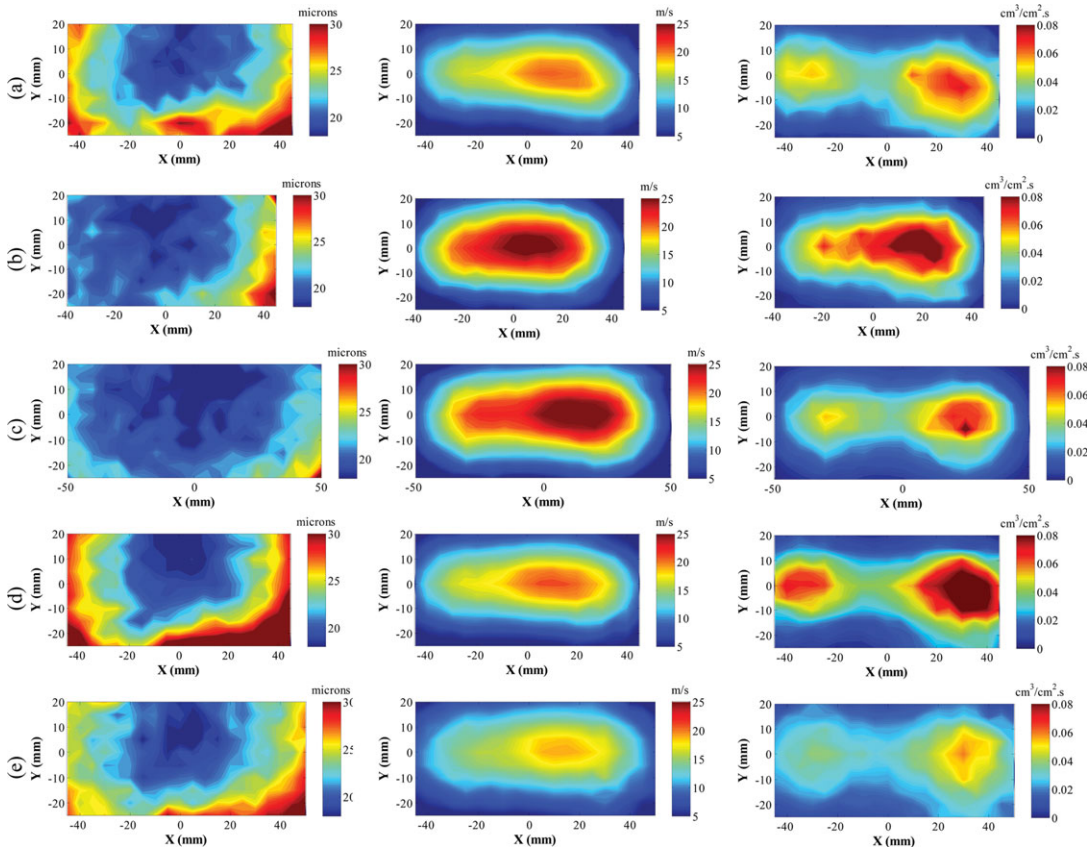

Figure 3. Diameter (D_{32}) (left), velocity (middle), and volume flux (right) data for Atomizer B sprays.

(a)–(e) show data for spraying conditions 1b–5b, respectively. [Color figure can be viewed in the online issue, which is available at wileyonlinelibrary.com.]

describe the influence of operating conditions (atomizing and shaping air supply pressure, liquid supply rate, gun-to-target distance, and formulation concentration) on spray characteristics, but also the different atomization characteristics resulting from the different gun designs.

Drop size (D_{32}) data, for instance, give information on key factors influencing atomization and drop transport. In particular, data show that the drop size distribution for atomizer A sprays was markedly different from those for the remaining four sprays. For atomizer A sprays, the smallest

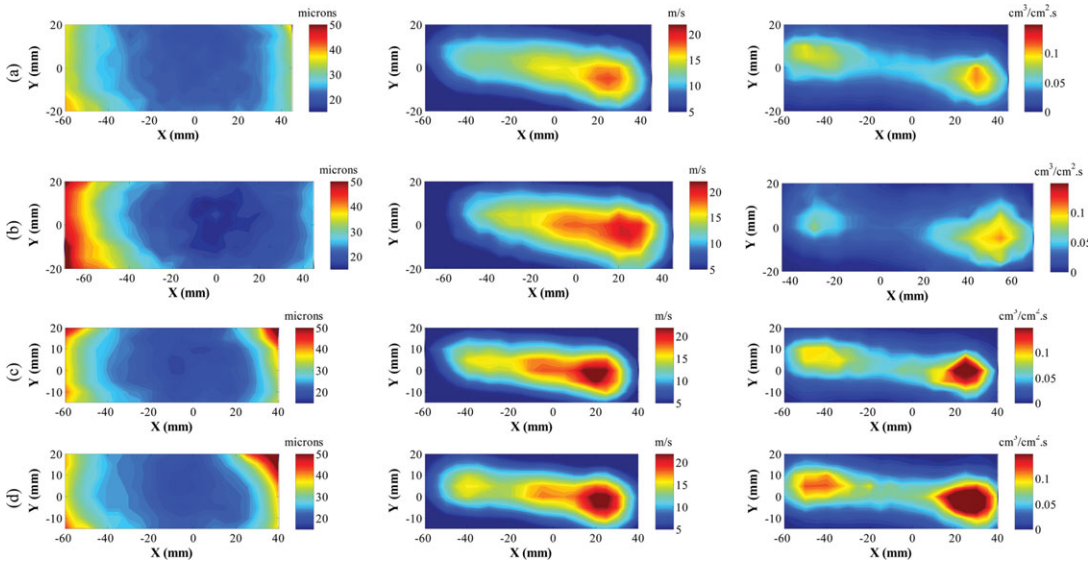

Figure 4. Diameter (D_{32}) (left), velocity (middle), and volume flux data (right) for Atomizer C sprays.

(a)–(d) show data for spraying conditions 1c–4c, respectively. [Color figure can be viewed in the online issue, which is available at wileyonlinelibrary.com.]

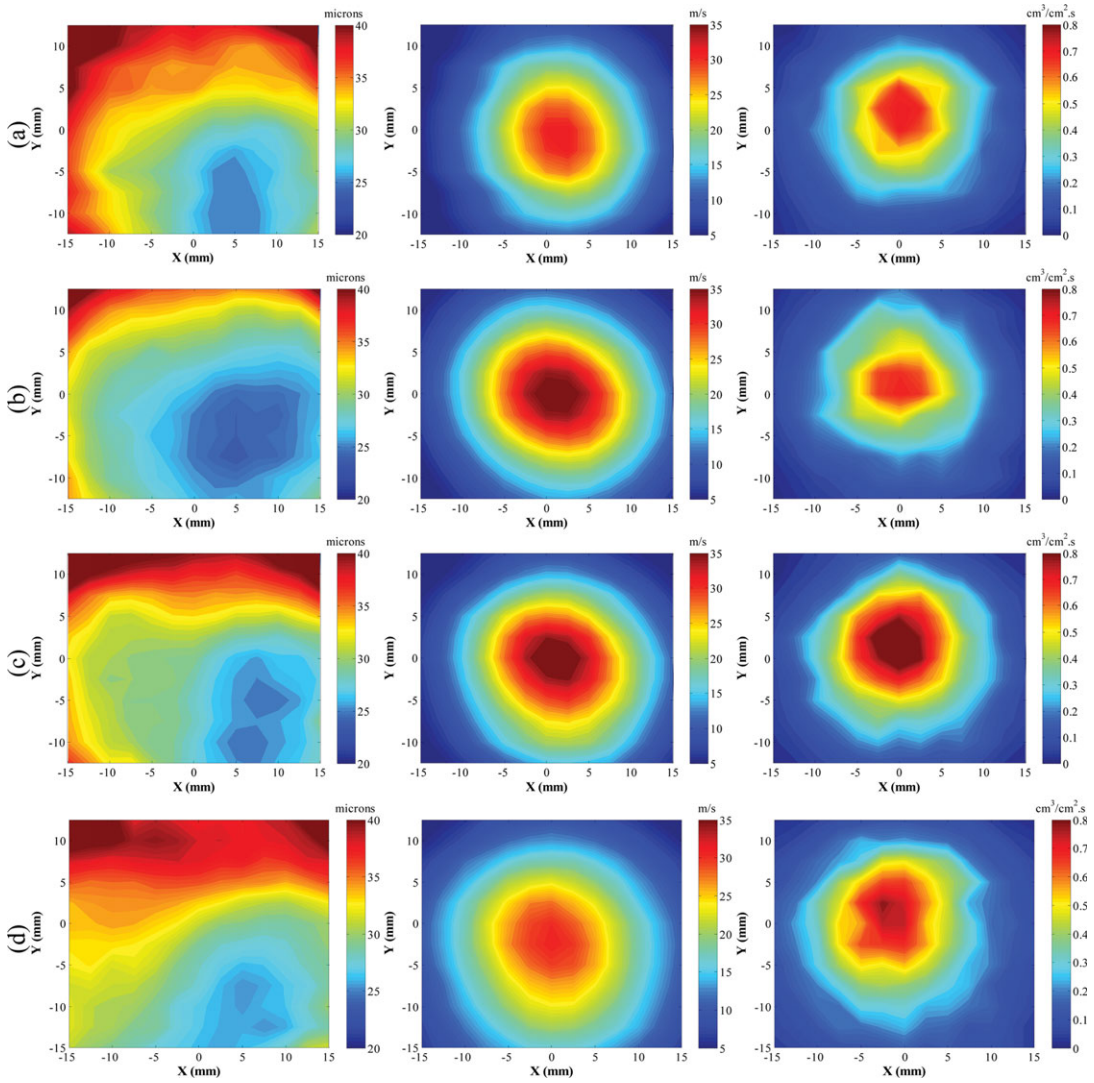

Figure 5. Diameter (D_{32}) (left), velocity (middle), and volume flux data (right) for Atomizer D sprays.

(a)–(d) show data for spraying conditions 1d–4d, respectively. [Color figure can be viewed in the online issue, which is available at wileyonlinelibrary.com.]

drops were clustered at two opposing ends of the spray semi-minor axis—where the shaping air flowed—while the remaining sprays had their smallest drops clustered approximately at the spray center.

Clustering of small drops at the spray center is a well-known behavior of air-assist sprays. It is the result of the ballistic nature of the large drops, which are more likely to resist the entrained air-induced drag that might move them toward the spray center. Accordingly, this behavior is expected for sprays whose primary means of atomization and drop transport are due to atomizing air. They include the two round sprays (atomizers D and E). Under the operating conditions used, atomizers B and C—with their atomizing air velocities greater than or equal to their shaping air velocities—are also likely to fall into this category. Atomizer A sprays, on the other hand, do not fall into this category as their shaping air velocity is twice as high as their atomizing air velocity. These conditions make atomizer A sprays unique in the following ways. First, their shaping air-induced secondary atomization will likely be as dominant a mechanism of atomization as that due to the atomizing air. Second, the small drops formed from all atomization processes will be more likely to follow the shaping air. Both factors ultimately led to the drop size distributions in Figure 2.

How gun design further influenced drop transport is also evident in the volume flux (patternation) and velocity data presented in Figures 2–6. With no shaping air flows present, the round sprays (Figures 5 and 6) exhibited largely axisymmetric patterns—with both the volume flux and velocity distributions resembling the expected profile of a round free jet—regardless of operating condition. Deviation from axisymmetrical patterns as a result of the shaping air flows are obvious from the volume flux and velocity data shown in Figures 2–4. More importantly, the same data also show that each of the flat sprays responded differently to changes in shaping air flow.

Atomizer B sprays transformed from a dumbbell to a teardrop pattern as atomizing air pressure rose. The dumbbell pattern was likely the result of spray "pinching" that occurred due to the shaping air flows. This effect was observed whenever the radial momentum along the spray semi-minor axis (due to shaping air) approached that of the downward momentum (due to atomizing air). Note that

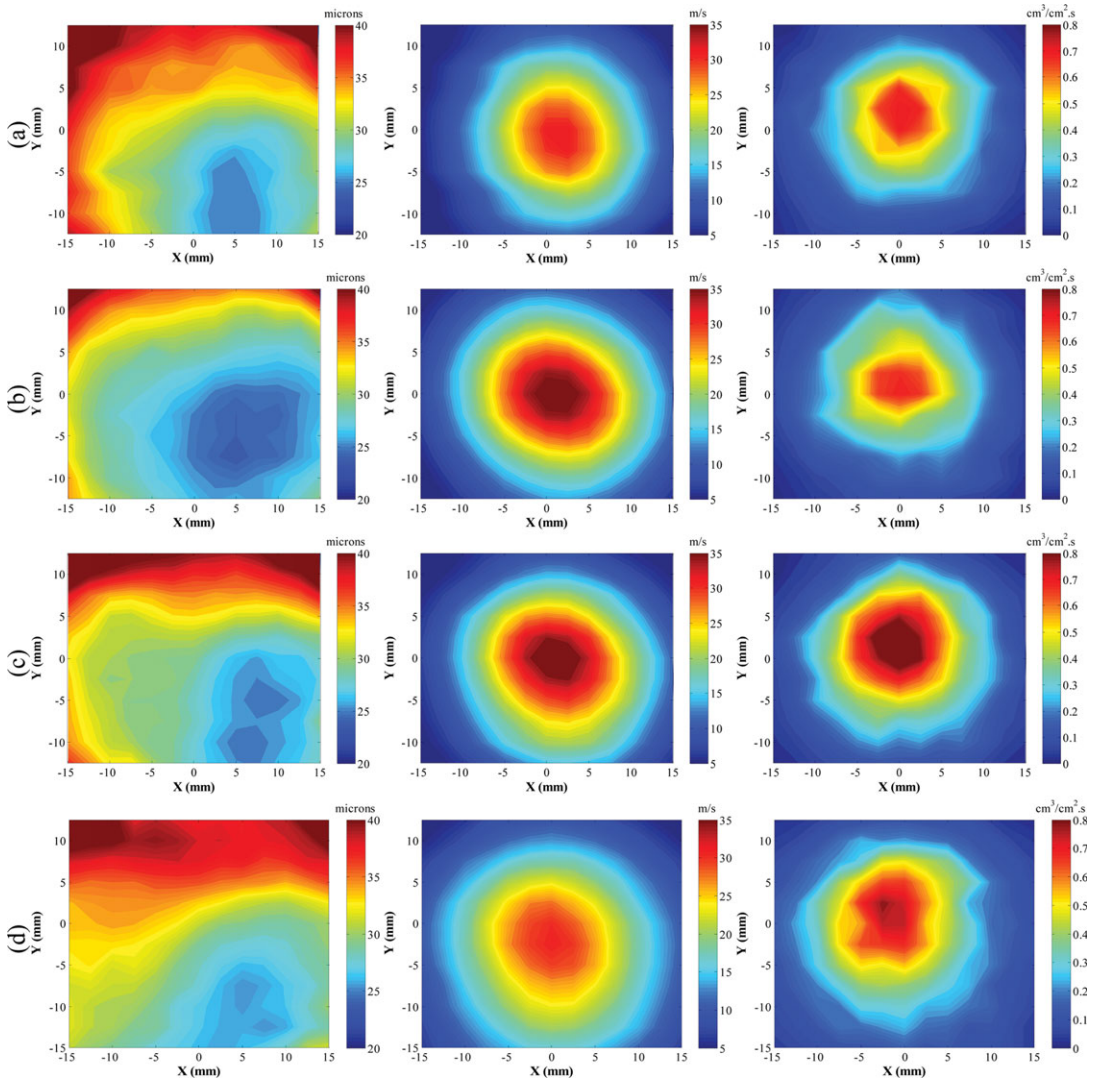

Figure 6. Diameter (D_{32}) (left), velocity (middle), and volume flux data (right) for Atomizer E sprays.

(a)–(d) show data for spraying conditions 1e–4e, respectively. [Color figure can be viewed in the online issue, which is available at wileyonlinelibrary.com.]

regardless of the shape of the spray patterns, the right side always appeared larger than the left (see second and third columns of Figure 3). This suggests that the axis of the shaping air channels was not aligned with the axis of the atomizing air channel; the former was likely several millimeters offset from the latter.

Volume flux profiles for atomizer C sprays were always dumbbell-shaped, regardless of operating conditions. In addition, similar to atomizer B sprays, the right side of atomizer C sprays was always larger than the left. Both observations are attributed to the explanations provided above. Furthermore, unlike atomizers A and B sprays, which decreased in width with increasing atomizing air pressure (this will be discussed in more detail in subsequent sections), atomizer C sprays increased in width when atomizing air pressure increased. This is because Atomizers A and B shaping air channels are independent of one another while the shaping air channel of atomizer C is interconnected with its atomizing air channel. Hence, increasing atomizer C air pressure would result in an increase in both atomizing and shaping air velocities. The increase in shaping air velocity in turn increased the spray width.

Of most interest is the observation that atomizer A sprays were less likely to produce dumbbell-patterned sprays than atomizers B or C sprays. In fact, volume flux data in Figure 2 show that atomizer A spray pattern was fairly uniform (i.e., no distinct localized peaks) when the gun was operated at the lower atomizing air pressure (205 kPa), the higher shaping air pressure (210 kPa), or the higher liquid supply rate (110 g/min). As atomizing air pressure rose, however, the spray became rounder and developed a peak at its center (third column of Figure 2b). To explain these observations, we first compare the shaping and atomizing air velocities, as well as the design of the three different guns.

PIV measurements/CFD simulations show that the shaping air velocities of the three different guns are approximately equal ($\sim$200 m/s at the outlets). The atomizing air velocity of atomizer A is 140 m/s, half that of atomizers B and C. Atomizers A and B share the same air cap design, but the atomizer C cap design is markedly different than those for atomizers A and B (see Figure 1). Finally, the shaping air channel of atomizer A is approximately three times as large that of atomizers B and C.

The dumbbell-shaped sprays produced by atomizer C were likely the result of the cap design. Compared to the flat caps on atomizers A and B, the horn cap on atomizer C was shaped such that the shaping air outlets were closer to the location where the shaping air flows meet (referred to hereafter as the junction point), and that the junction point was located further downstream from the atomizing air outlet (see Figure 1). Hence, although atomizer C had similar shaping and atomizing air velocities as atomizer B, atomizer C sprays were exposed to higher shaping air velocity but lower atomizing air velocity at the pinching point. Such a condition made pinching more likely, as observed from Figure 5 data. Nevertheless, dumbbell-patterned sprays could likely be avoided had the atomizer allowed separate adjustments of atomizing and shaping air pressures.

Although the flat cap design and the separate atomizing/shaping air controls contribute to the production of more uniform and non-dumbbell shaped sprays, what truly makes atomizer A unique is the gun's lower atomizing air velocity and its larger shaping air channels. Due to the former, atomizer A-produced D_{32} was as large as 45 μm when operated without the shaping air flows; twice as large as atomizer B sprays produced under the same atomizing air pressure and liquid supply rate. The larger drops upstream of the junction point made atomizer A sprays significantly more susceptible to shaping air-induced secondary atomization. The larger shaping air channels further promoted this effect by providing more energy for atomization. These two claims are supported by the drop size data in Figure 2, as discussed earlier.

Having more significant secondary atomization at the spray junction point nullified the pinching effect that would otherwise take place—as in the case of atomizers B and C—and instead made the spray more uniform. This hypothesis also explains why conditions that increase drop size upstream of the junction point—which would make the drops more susceptible to secondary atomization—such as increasing the liquid supply rate, increasing the shaping air pressure, or decreasing the atomizing air pressure, tend to make the spray more uniform, as observed in Figure 2 volume flux data.

The effects of individual gun operating parameters on drop size, velocity, volume flux, and pattern are now discussed. It is important to note that since the sprays total volume flux is independent on operational parameters other than the liquid supply rates, discussions related to volume flux quantities presented in subsequent sections pertain only to local volume flux magnitudes—i.e., volume flux quantities at specific locations within the spray cross-sectional area—and how they vary with gun operating parameters. For the external-mix sprays, the operating parameters considered include atomizing air supply pressure, liquid supply rate, gun-to-target distance, formulation concentration, and exclusively for atomizers A and B, shaping air pressure. Spray data for internal mix sprays are presented in terms of air-to-liquid mass ratio (ALMR), gun-to-target distance, and formulation concentration.

The influence of atomizing air pressure on spray characteristics

The effects of increasing atomizing air pressure on drop size (D_{32}), axial velocity, and volume flux can be seen by comparing Figures 2a, b for atomizer A spray (conditions 1a and 2a), Figures 3a, b for atomizer B spray (conditions 1b and 2b), Figures 4a, b for atomizer C spray (conditions 1c and 2c), and Figures 5a, b for the atomizer D spray (conditions 1d and 2d).

Diameter data for all sprays show that drop diameter decreased as atomizing air pressure increased. This behavior was the result of an increase in the air-to-liquid mass ratio and the relative velocity between the air and the liquid, both of which provided finer atomization.

The middle columns of Figures 2a, b–5a, b show the corresponding velocity maps. An increase in drop velocity occurred when atomizing air pressure rose for all sprays. Such an increase was expected, as increasing atomizing air supply pressure increased the momentum rate of air transporting the drops downstream.

Atomizers A and B velocity data (Figures 2a, b and 3a, b) suggest that a less elliptical spray was produced following an increase in atomizing air supply pressure. This may be due to the reduction in drop size, along with the realization that smaller drops are more susceptible to entrained air-induced drag force that drives them towards the spray center. In addition, the atomizing air also provides downward (axial) momentum for the droplets. Increasing drop axial velocity in turn lessens the spreading effect induced by the shaping air.

The reduction in spray extent is supported by the volume flux data shown in the rightmost column of Figures 2a, b and 3a, b. Note that the local volume flux magnitude for all sprays was typically highest near the location where the drop velocity was highest. This was expected, and as noted above, is because volume flux is proportional to drop velocity. Accordingly, local volume flux for all sprays increased as atomizing air pressure increased.

In contrast to atomizers A, B, and D spray data, atomizer C data show that spray pattern widened slightly as atomizing air supply pressure rose. This observation is the result of interconnecting atomizing and shaping air channels, as previously explained. Note that this behavior was not observed in the remaining elliptical sprays because the guns that produced them (A and B) have separate controls for the shaping and atomizing air.

Finally, contrary to the three elliptical sprays, the volume flux profiles for the atomizer D sprays were insensitive to changes in atomizing air pressure, as evident from Figure 4a, b. Here, it can be observed that the increase in air-to-liquid mass ratio did not affect local volume flux values. This suggests that the decrease in volume flux due to the decrease in drop size was balanced out by the increase in volume flux due to the increase in velocity.

The influence of shaping air pressure on spray characteristics

The influences of shaping air pressure on drop size (D_{32}), axial velocity, and volume flux can be seen by comparing Figures 2b–c for atomizer A sprays (conditions 2a and 3a), and by comparing Figures 3b–c for atomizer B sprays (conditions 2b and 3b). Figures 3b, c show that drop diameter decreases as shaping air pressure increases. This is due to secondary atomization. Supporting this claim are the shaping air velocity magnitude for atomizer B and the sprays D_{32} values for condition 2b. The former was approximately 260 m/s, as noted above, whereas the latter was $\sim$18 μm. These numbers translate to a Weber number of $\sim$20, well above the critical value for drop secondary breakup (We $\sim$12).

Note that the decrease in size accompanying the increase in shaping air pressure for atomizer A sprays was much more

significant than that for atomizer B sprays—the decrease in atomizer B spray size due to the increase in shaping air pressure was only observed at locations close to the spray center, whereas the decrease was observed throughout the entire spray cross-sectional area for atomizer A sprays. This observation further exemplifies the point that atomizer A sprays were more susceptible to secondary atomization than atomization B sprays. As previously noted, this is due to spray A's larger drops upstream of the junction point (due to the gun's lower atomizing air pressure) and the gun's larger shaping air channels.

The expected development of more elliptical sprays can be observed from the volume flux and velocity data in Figures 2c and 3c. For atomizer A sprays, the increase in spray width was also accompanied by the development of a more uniform spray (no distinguishable peaks), whereas for atomizer B sprays, it was accompanied by the development of dumbbell-shaped sprays. The former was the result of shaping air-induced secondary atomization becoming significantly more dominant than shaping-air induced spray pinching. The opposite took place in the latter case. Both cases have already been explained in the preceding paragraphs.

For the atomizer A spray, an increase in shaping air pressure led to a slight decrease in drop velocity. This result was unexpected, but is likely due to the contribution of two factors. The first is the junction point dynamics that led to the decrease in drop size with increasing shaping air pressure. The second is the measurement location; as listed in Table 3, both condition 2a and 3a data were collected at 14 cm downstream of the nozzle tip. At such a distance the momenta due to the shaping and atomizing air jets had likely dissipated, and the spray evolution process became dominated by drop deceleration due to them moving in a quiescent surrounding. As smaller droplets lose their momentum more rapidly, they decelerate more quickly. This would lead to the observed decrease in velocity. It should be noted that Scattergood et al.[18] reported similar behavior. In contrast to the atomizer A spray, an increase in shaping air pressure slightly increased drop velocity for the atomizer B spray. This is likely due to the decrease in drop size accompanying an increase in shaping air pressure for atomizer B spray being less significant and not as observable throughout as for the atomizer A spray.

The influence of air-to-liquid mass ratio (ALMR) on spray characteristics (internal mix sprays)

The influence of decreasing air-to-liquid mass ratio (ALMR) on drop size (D_{32}), axial velocity, and volume flux for atomizer E (internal mix) sprays can be observed by comparing the first three rows in Figure 6 (spraying conditions 1e–3e). ALMR was decreased by increasing liquid supply pressure first from 205 to 275 kPa (conditions 1e–2e), and finally to 345 kPa (condition 3e), while keeping the air supply pressure fixed.

Figures 6a–c data suggest that increasing the liquid supply pressure from 205 to 275 kPa had little effect on drop size or velocity, but raising it past 275 kPa increased drop size and decreased drop velocity. This suggests that relatively constant drop size and velocity can be achieved by operating above a certain level of ALMR.

The asymptotic decrease in size with increasing ALMR is a widely known behavior of air-assist sprays,[38–40] and can be explained as follows. First, for atomization due to shear breakup in high-speed gas streams, drop diameter is linearly proportional to the Rayleigh-Taylor instability wavelength, λ_{RT}, the fastest growing instability wavelength in a ligament and therefore the one that leads to drop formation. According to Varga et al.,[38] λ_{RT} for cases where air density is negligible compared to liquid density is

$$\lambda_{RT} = \frac{\kappa \xi}{(u_g - u_l) u_g^{1/4}} \tag{1}$$

where u_g and u_l are, respectively, the gas and liquid velocity, κ is a proportionality constant that accounts for the specifics of the nozzle geometry, and ξ is a constant determined by the fluid properties

$$\xi = \sigma^{1/2} \left(\frac{v_g \rho_l}{\rho_g^3} \right) \tag{2}$$

Here, σ is the liquid surface tension and v_g, ρ_l, and ρ_g are the gas kinematic viscosity, liquid density, and gas density, respectively.

As both the atomizer geometry and fluid properties were not varied in conditions 5a-c, variations in λ_{RT} will depend only on the gas and liquid velocities. From Eq. 1, it is obvious that λ_{RT} decreases—therefore drop size decreases—as liquid velocity decreases. However, at low enough liquid velocity, only u_g is important and λ_{RT} scales only with $u_g^{-5/4}$. Taking this into account, and realizing that the spraying conditions are such that air supply pressure (therefore air velocity) remained constant, λ_{RT}, and correspondingly drop size, will approach a constant minimum as liquid supply pressure (velocity) falls below a certain level, leading to the observed size data in Figures 6a–c.

Drop velocity data in Figures 6a–c can be explained by first considering D_{10}, D_{20}, and D_{30} data in Figures 7a, b. Here, it can be seen that for spraying conditions 1e and 2e, the three diameter statistics differ by at most 20% and D_{10} for both conditions is $\sim$10 μm throughout most of the entire spray area. This suggests that the sprays produced under conditions 1e and 2e consist of mostly small ($\sim$10 μm) drops. Since a 10 μm water droplet requires only $\sim$25 μs to get accelerated to 99% of the surrounding gas velocity, it is likely that at the gun-to-target distance where the measurements were taken (10 cm downstream of the gun tip, at which point the atomizing air jet was still likely to influence the spray evolution process), most of the drops had already achieved the gas phase velocity, which is the same for spraying conditions 1e and 2e. This then led to the nearly identical drop velocity distributions observed in Figures 6a, b.

As ALMR decreased to condition 3e, however, larger drops were produced (see Figures 6c and 7c size data). Larger drops would not reach the gas phase velocity as rapidly as smaller ones would. This led to the decrease in drop velocity observed in Figure 6c.

As mentioned earlier, decreasing ALMR by switching from spraying condition 1e–2e did little to drop size and velocity, yet the rightmost column of Figures 6a, b suggests that doing so increased local volume flux magnitude. This was expected since ALMR was reduced by increasing liquid supply rate, and was likely the result of an increase in drop concentration, in accordance with the PDA detection rate data in Figure 8. Switching from spraying condition 2e–3e further increased local volume flux magnitude. This was likely due to the production of larger drops.

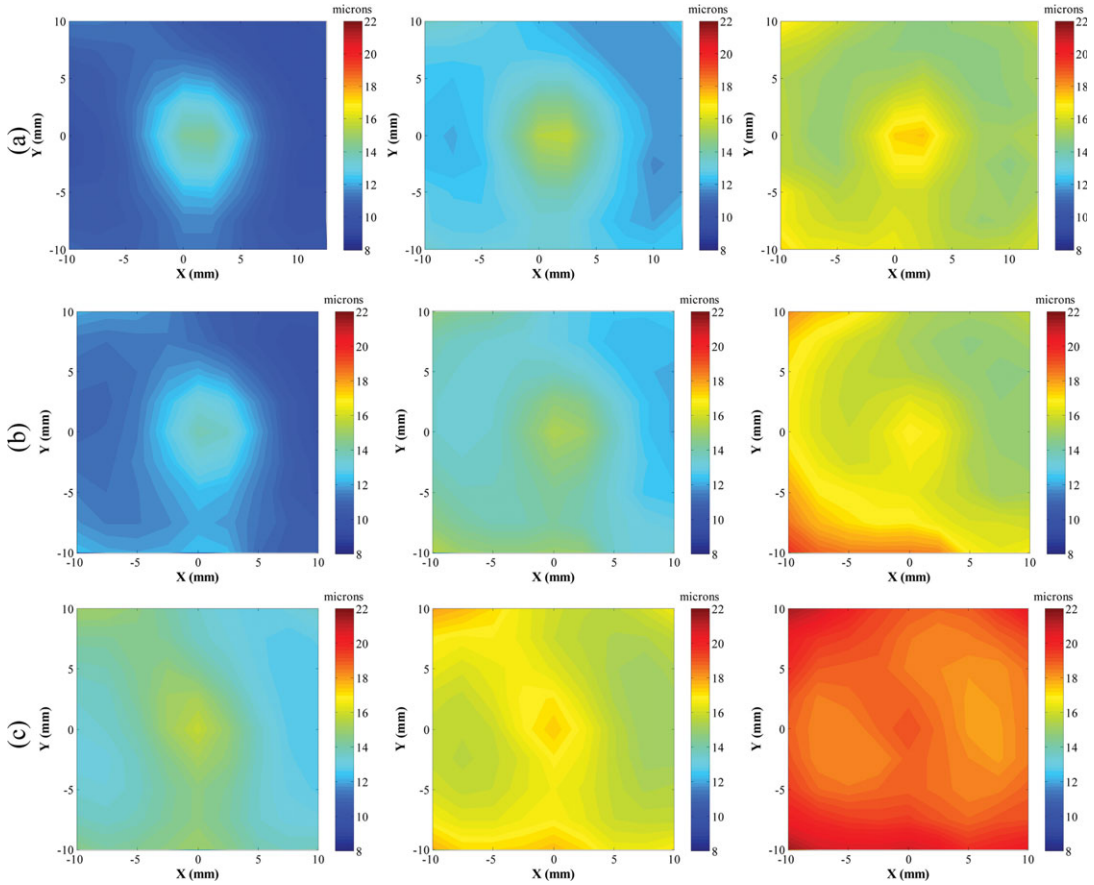

Figure 7. D_{10} (left), D_{20} (middle), and D_{30} (right) data for Atomizer E sprays.

From top to bottom, spraying conditions are 1e, 2e, and 3e. [Color figure can be viewed in the online issue, which is available at wileyonlinelibrary.com.]

The influence of liquid supply rate on spray characteristics

The effects of increasing liquid supply rate on spray characteristics can be seen by comparing Figures 2b–d for atomizer A sprays (conditions 3a and 4a), Figures 3a–d for atomizer B sprays (conditions 1b and 4b), Figures 4c–d for atomizer C sprays (conditions 2c and 3c), and Figures 5b, c for atomizer D sprays (conditions 2d and 3d). Drop size (D_{32}) data for all sprays show an increase in drop size, particularly at the spray periphery, as liquid supply rate increased. The formation of larger drops was expected, and was due to the decrease in both air-to-liquid mass ratio and the relative velocity between the air and the liquid.

It should be noted that the increase in drop size following an increase in liquid supply rate was most pronounced for atomizer A sprays. This is because, under the operating conditions tested, the atomizing air velocity of atomizer A was much lower than that of other atomizers. Atomizer A therefore provided less efficient primary atomization and its sprays would in turn be more sensitive to the effects of an increase in liquid supply rate on drop size (see Eq. 1).

Drop velocities for all sprays decreased as liquid supply rate increased. This is expected for two reasons. First, the increase in liquid mass was not balanced by an increase in total air mass flow rate so less air per unit mass of liquid was available to transport the droplets downstream. The

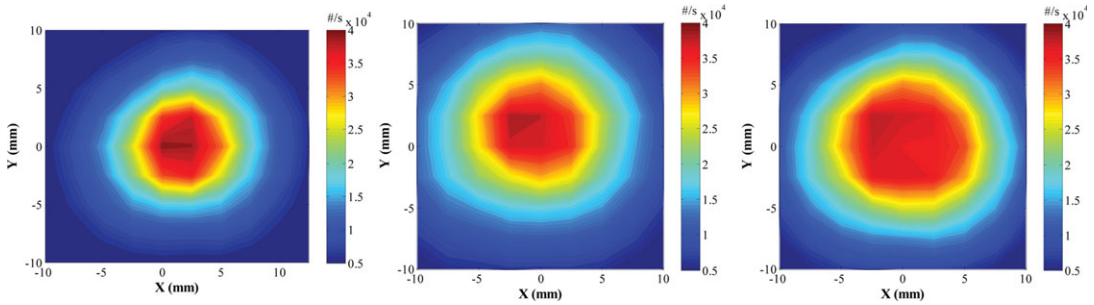

Figure 8. PDA detection rate data for Atomizer E sprays.

From left to right, spraying conditions are 1e, 2e, and 3e. [Color figure can be viewed in the online issue, which is available at wileyonlinelibrary.com.]

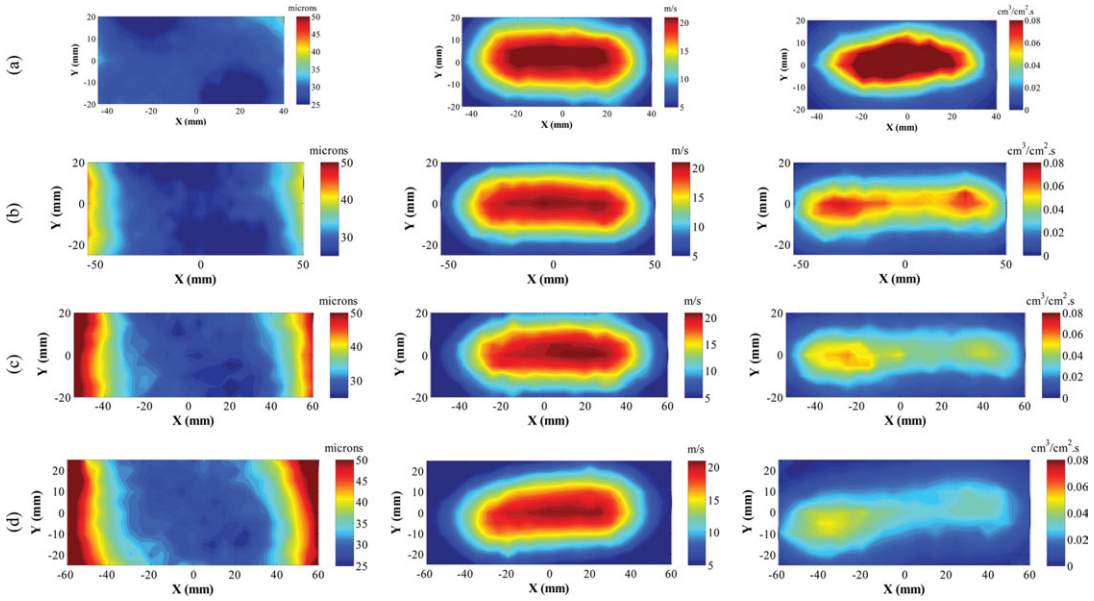

Figure 9. Diameter (D_{32}) (left), velocity (middle), and volume flux data (right) for Atomizer A sprays.

Formulations are (a) water (b) 1.5, (c) 2.5, and (d) 3.5% w/w HPMC-E5. [Color figure can be viewed in the online issue, which is available at wileyonlinelibrary.com.]

second reason is related to the production of larger drops, as explained earlier.

Velocity and volume flux profiles show that all sprays became wider as liquid supply rate rose. This is expected, since the larger drops produced at higher liquid mass flowrate were less prone to entrained air induced aerodynamic drag forces that might drive them toward the spray center. Note that for the elliptical sprays, spray widening was not axi-symmetric; it was evident only along their semimajor axis. This was due to the influence of the shaping air flows, which prevented the sprays to widen along the semiminor axis (where the shaping air flows). In addition to the increase in spray extent, local volume flux magnitude for all sprays increased with an increase in liquid mass flow rate. This too was expected since larger drops were being produced.

Volume flux and velocity results again show that the elliptical sprays responded differently to variations in liquid supply rate. For atomizers B and C, increasing the liquid supply rate simply made the spray more elliptical. The overall spray pattern, however, was unchanged and remained dumbbell-shaped. In contrast, for atomizer A spray, increasing the liquid supply rate made the spray somewhat more uniform, in addition to making the spray more elliptical. The explanation for this behavior is already provided above.

The influence of gun-to-target distance on spray characteristics

The effects of increasing gun-to-target distance on drop size (D_{32}), axial velocity, and volume flux can be seen by comparing Figures 2d, e for atomizer A spray (conditions 4a and 5a), Figures 3d, e for atomizer B spray (conditions 4b and 5b), Figures 4c, d for atomizer C spray (conditions 1c and 3c), Figures 5c, d for atomizer D spray (conditions 3d and 4d), and Figures 6c, d for atomizer E spray (conditions 3e and 4e). Drop size data for all sprays show that an increase in gun-to-target distance led to an insignificant increase in drop size. This suggests that the lab conditions under which the experiments were conducted promote very little drop evaporation. This observation, however, may not represent the actual tablet coating process as drum-coater drying air is often heated to $\sim 60^{\circ}$C during operation.

Velocity data show that an increase in gun-to-target distance decreased drop velocity. This observation was expected, and was the result of drop deceleration due to aerodynamic drag. Velocity data, along with spray volume data, also show the expected spray expansion following an increase in gun-to-target distance.

In addition, an increase in gun-to-target distance also decreased spray volume flux. This was expected considering both the decrease in drop velocity (recall again that volume flux is directly proportional to velocity) and spray expansion. Finally, it can be seen that, apart from increasing the spray extent, variations in gun-to-target distance had no significant effect on size, velocity, and volume flux profiles of all sprays (e.g., the location of maxima and minima in volume flux and velocity profile were unchanged).

The influence of formulation on spray characteristics

The influence of liquid rheology (via a change in formulation) on drop size (D_{32}), axial velocity, and volume flux for atomizer A sprays are shown in Figure 9. The spray condition is 2a. The same set of data, but for atomizer E sprays, are shown in Figure 10. The spraying condition is 3e. For both cases, liquid rheology was varied by modifying the concentration of an HPMC-E5 solution. The surface tension, density, and viscosity of the different HPMC-E5 mixes are summarized in Table 4.

From the leftmost columns of Figures 9 and 10, it is clear that drop size increased with an increase in formulation concentration. As the surface tensions and densities of the HPMC formulations were approximately equal, the increase in size must be the result of an increase in viscosity. This behavior was expected, as an increase in liquid viscosity helped oppose the hydrodynamic instabilities leading to ligament formation. As a result, when atomization does occur, it does so further downstream from the gun outlet where air velocity is relatively lower.

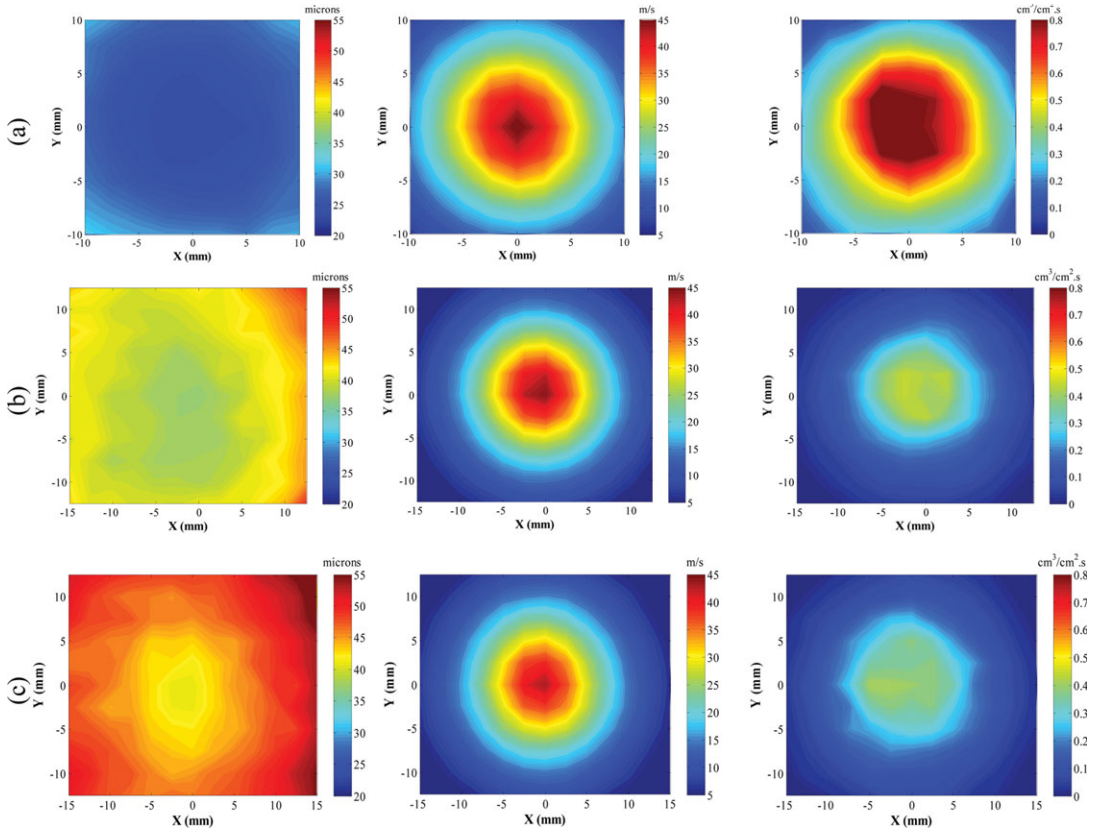

Figure 10. Diameter (D_{32}) (left), velocity (middle), and volume flux data (right) for Atomizer E sprays.

Formulations are (a) water, (b) 1.5, and (c) 3.5% w/w HPMC-E5. [Color figure can be viewed in the online issue, which is available at wileyonlinelibrary.com.]

Furthermore, an increase in liquid viscosity also helps oppose aerodynamic induced-breakup for secondary atomization dominated processes. Both effects would increase drop size.

The middle column of Figures 9 and 10 shows that an increase in formulation concentration slightly decreased drop velocity. This was again related to the production of larger drops, as explained earlier.

Accompanying the increase in drop size for atomizer A sprays was the development of more elliptical patterns. This was due to the reasons explained above. More importantly, however, it can be observed that the dumbbell-shaped pattern developed as the spray widened. This observation further signifies the importance of secondary atomization in homogenizing the sprays. As noted above, the increase in viscosity helped the drops oppose secondary breakup. With the drops becoming more difficult to break apart, the shaping air took the role of pinching, as in the case of atomizers B and C sprays. Note that, in cases where the dumbbell sprays were most apparent (Figures 9c, d), the unique drop size distribution seen in Figure 2 no longer appeared; drop size distributions of the spray instead became similar to those of spray B. This further supports the hypothesis that secondary breakup at the spray junction point became less significant when liquid viscosity increased—which ultimately made shaping air-induced spray pinching more likely to occur.

Figure 9 data also show that local volume flux magnitude decreased as formulation concentration increased. This observation is the result of two effects. First is the decrease in local spray concentration. The decrease in spray concentration is the result of the increase in size that was not accompanied by significant change in drop velocity and liquid supply rate. It is confirmed by the PDA data rate data shown in Figure 11. A decrease in spray concentration means that the average number of drops per unit area (and per unit volume) decreases. This, when combined with the development of a wider and more elliptical spray, resulted in a decrease in local spray volume flux, as observed in Figure 9.

Increasing formulation concentration for atomizer E sprays also increased spray coverage and slightly changed the overall volume flux profile. Compared to water sprays, HPMC-E5 sprays were wider and more uniform (their volume flux peak wasn't as apparent as that for water sprays). Both HPMC-E5 and water sprays, however, had similar circular profiles.

Similar to atomizer A HPMC-E5 sprays, evidences of a decrease in spray concentration were also observed for atomizer E HPMC-E5 sprays (Figure 12). The development of wider sprays, combined with the aforementioned decrease in spray concentration, resulted in a decrease in local volume flux magnitude, again mirroring the behavior of atomizer A sprays.

Table 4. Density, Surface Tension, and Viscosity of Different HPMC-E5 Mixes

Formulation	Density (kg/m^3)	Surface Tension (dynes/cm)	Viscosity (mPa.s)
0% w/w HPMC-E5 (water)	996	76.5	0.98
0.5% w/w HPMC-E5	996	52.5	1.90
1.5% w/w HPMC-E5	997	51.7	4.17
2.5% w/w HPMC-E5	998	51.5	6.40
3.5% w/w HPMC-E5	999	51.7	8.09

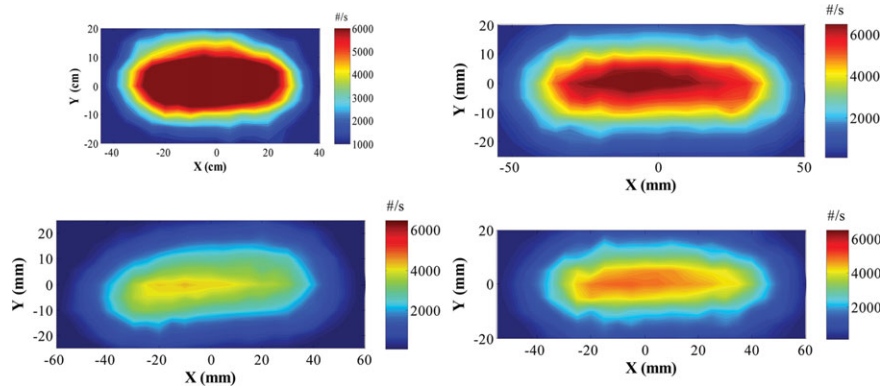

Figure 11. PDA detection rate for Atomizer A sprays.

Formulations, clockwise from top left, are water, 1.5, 2.5, and 3.5% w/w HPMC-E5 sprays. [Color figure can be viewed in the online issue, which is available at wileyonlinelibrary.com.]

The influence of atomizer wear on spray characteristics

During extensive usage and handling, the liquid cap of atomizer D developed a small dent at its tip (see Figure 13). Information on how such a dent influences spray characteristics is important, as pharmaceutical nozzles are often exposed to similar usage and handling. For this reason, sprays produced by the damaged gun were characterized. Data are presented as Figure 14. Spraying conditions are 1d and 2d.

Comparison of Figures 14a to 5a and 14b to 5b shows that gun wear significantly influenced spray characteristics, especially drop size (D_{32}) and drop velocity profiles. Sprays produced while using the damaged liquid cap were smaller in drop size, and their smallest drops were centered at the spray periphery. In contrast, sprays produced by the undamaged liquid cap had their smallest drops clustered near the spray center. The damaged gun drop velocities also had an elliptical profile, as opposed to the circular drop velocity profiles produced by the undamaged gun.

The above observations can be explained by considering the CFD results in Figure 15. Here, the "Volume-of-Fluid" method was used to track the liquid/gas interface at the atomizing lip. The direction of the liquid jet and the atomizing air flow is upward. As shown, the dent in the liquid cap tip changed the direction in which half of the atomizing air flow exited the gun. As a result, drops were likely formed due to pinching, instead of shearing, of the ligament. This likely led to the production of the smaller drops observed in Figure 14. In addition, the angled atomizing air flow also likely "pushed" the small drops, which are more easily influenced by the surrounding air flows, to the spray periphery. It could also have led to the elliptical velocity profiles observed in Figure 14.

Summary and Conclusions

Measurements show that there are spatial variations in drop size, velocity, and volume flux for sprays produced by typical pharmaceutical coating guns. These spatially resolved quantities in turn show how sprays respond to changes in operating conditions and gun characteristics in ways that less complete measurements could not provide. For instance, the effects of increasing liquid supply rate on the size distribution of atomizer B ("small" external mix gun, with flat-shaped/antibearding cap assembly) sprays would have been underestimated had the measurements been performed only along a spray axis, as size variations due to the liquid supply rate for this gun occur only at the spray corners. The effects of gun wear on spray characteristics would also likely not be identified had the measurements been performed at only few points across the sprays. Finally, measurements along a spray axis would also fail to recognize the unique drop size distribution of spray A ("large" external mix gun, with flat-shaped/antibearding cap assembly), which was important in determining the dual roles of the shaping air flow—arguably the most important finding from this study.

Depending on drop size upstream of the junction point (the location where the shaping air flows meet), the drop

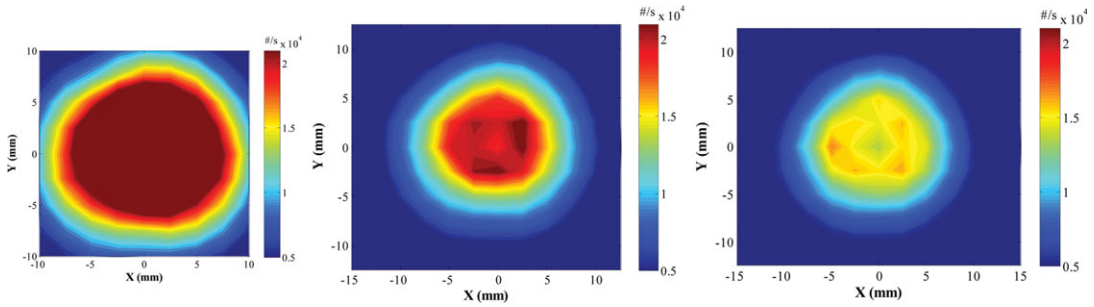

Figure 12. PDA detection rate for Atomizer E sprays.

Formulations, from left to right, are water, 1.5, and 3.5% w/w HPMC-E5 sprays. [Color figure can be viewed in the online issue, which is available at wileyonlinelibrary.com.]

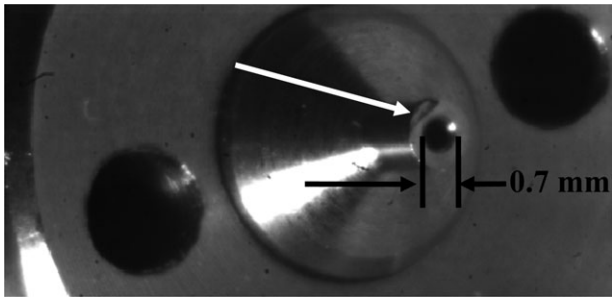

Figure 13. Photograph of the damaged Atomizer D liquid cap.

Note dent marked by arrow.

viscosity, and the magnitude of the shaping air velocity, the shaping air can either pinch or induce secondary atomization to the sprays. When the former outweighs the latter, a dumbbell-shaped spray develops; a more uniform spray results when the opposite takes place.

Atomizer A, which under the operating conditions tested had the lowest atomizing air velocity, produced considerably larger drops upstream of the pinching point than the other flat sprays. Larger drops are more susceptible to secondary breakup. This, combined with the gun's larger shaping air channel, resulted in the shaping air flow taking the role of homogenizing the spray. Atomizers B and C (external mix gun with horn-shaped cap assembly), on the other hand, operated under the criteria that would promote spray pinching.

A corollary to the proposed hypothesis is that pinching would occur when factors prohibiting secondary atomization are enforced. This was confirmed by the development of dumbbell-shaped sprays following an increase in viscosity—a factor that inhibits secondary breakup. It should be noted that whether secondary atomization would homogenize the sprays or pinch them may be related to the Ohnesorge number-corrected Weber number[41] calculated from the drop sizes upstream of the pinching point, drop viscosity, and the shaping air velocity at the pinching point. This, however, must be confirmed through further experiments.

Spatially resolved data show that the elliptical sprays were sensitive to changes in shaping air pressure, atomizing air pressure, liquid supply rate, formulation viscosity, and gun design. In contrast, round sprays were not sensitive to those operating conditions. In fact, data show that the round sprays became *more* uniform, as a result of a decrease in drop concentration at the spray center, with increasing liquid viscosity. A practical implication of this finding is that a more robust and consistent pharmaceutical tablet coating process can likely be designed by utilizing multiple round sprays that are uniformly spaced so that they overlap.

Spatial variations aside, data show that the behaviors of typical pharmaceutical nozzles are similar to those of general air-blast sprays. They include:

- An increase in mean drop size with a decrease in atomizing air pressure, an increase in liquid supply rate, an increase in gun-to-target distance, or an increase in formulation concentration.
- Exclusively for atomizers A and B sprays, an increase in shaping air pressure also decreases mean drop size.
- An asymptotic decrease in drop size with an increase in air-to-liquid mass ratio (ALMR) for the internal mix sprays.
- An increase in drop velocity following an increase in atomizing air pressure or a decrease in liquid supply rate.
- An increase in local volume flux magnitude following an increase in liquid supply rate, an increase in atomizing air pressure, a decrease in shaping air pressure, or a decrease in formulation concentration.
- Sprays that generally widen as shaping air pressure increases or as drop size increases (i.e., as liquid supply rate or formulation concentration is increased, or as atomizing air pressure is decreased).

Many of the previous observations have been reported by Lefebvre[42] and references therein.

It should be noted that, although this study successfully identifies the key operating conditions and gun

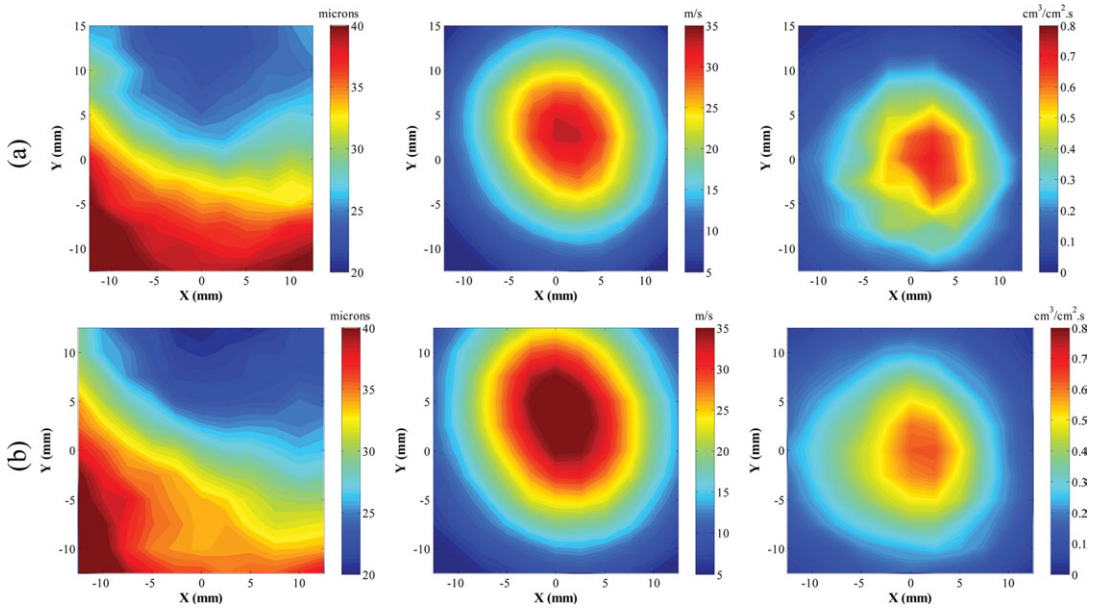

Figure 14. Diameter (D_{32}) (left), velocity (middle), and volume flux data (right) for the "damaged" Atomizer D sprays.

Spraying conditions are conditions (a) 1d and (b) 2d. [Color figure can be viewed in the online issue, which is available at wileyonlinelibrary.com.]

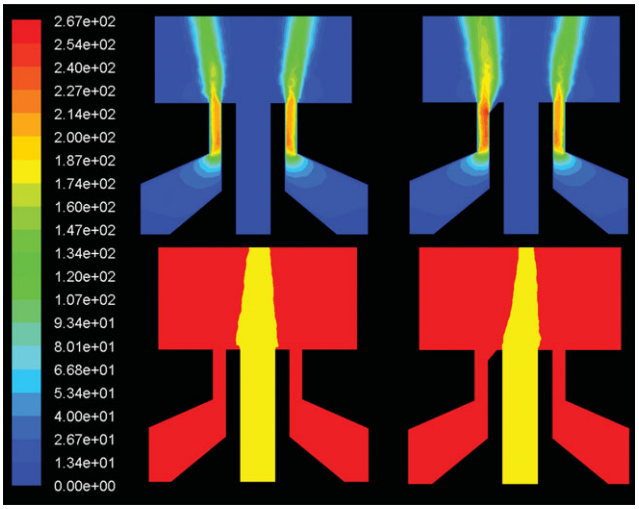

Figure 15. Computed atomizing air velocity from an undamaged (left) and a damaged (right) Atomizer D gun tip.

The corresponding volume fraction of the gas (red) and the liquid (yellow) are shown in the second row. [Color figure can be viewed in the online issue, which is available at wileyonlinelibrary.com.]

characteristics responsible for homogenizing the sprays, it does not account for spray evolution due to the influence of coating drum parameters such as rotational speed and drying air flow. As such, process guidelines derived from this study alone will not ensure quality-by-design for the spray tablet coating processes. More inclusive guidelines should account for the influence of coating drum parameters. They can be provided via PDA drop size/velocity/volume flux measurements of sprays in a drum coater and/or via simulations using a CFD model. One taking the modeling approach can describe the sprays by coupling a Lagrangian discrete phase tracking algorithm with the Eulerian (continuous) phase. Spatially resolved spray data such as those presented here can be used as the initial conditions for the discrete phase. A successful implementation of this strategy will yield sprays characteristics and patterns at the tablet bed—subsequent to them being influenced by the drum drying air and rotation. Both the experimental and computational approaches should be considered in future spray tablet coating studies.

Literature Cited

1. Kim S, Mankad A, Sheen P. The effect of application rate of coating suspension on the incidence of the bridging of monograms on aqueous film-coated tablets. *Drug Dev Ind Pharm*. 1986;12:801–809.
2. Rowe RC, Forse SF. The effect of plasticizer type and concentration on the incidence of bridging of intagliations on flm-coated tablets. *J Pharm Pharmacol*. 1981;33:174–175.
3. Twitchell AM. Studies on the Role of Atomisation in Aqueous Tablet Film Coating. PhD Thesis, Leicester, United Kingdom: Leicester Polytechnic, 1990.
4. Twitchell AM, Hogan JE, Aulton ME. The effect of atomizing air pressure on the aqueous film coating process and on film coat quality. Presented at the 1st World Meeting on Pharmaceutics, Biopharm, Budapest, May 9–11, 1995.
5. Reiland TL, Eber AC. Aqueous gloss solutions—formula and process variables effects on the surface texture of film coated tablets. *Drug Dev Ind Pharm*. 1986;12:231–245.
6. Ruotsalainen M, Heinamaki J, Taipale K, Yliruusi J. Influence of the aqueous film coating process on the properties and stability of tablets containing a moisture-labile drug. *Pharm Dev Technol*. 2003;8:443–451.
7. Fisher DG, Rowe RC. Adhesion of film coatings to tablet surfaces—instrumentation and preliminary evaluation. *J Pharm Pharmacol*. 1976;28:886–889.
8. Rowe RC. The adhesion of film coatings to tablet surfaces—a problem of stress distribution. *J Pharm Pharmacol*. 1981;33:610–612.
9. Rowe RC, Forse SF. The effect of process conditions on the incidence of bridging of the intagliations and edge splitting and peeling on film coated tablets. *Acta Pharm Technol*. 1982;28:207–210.
10. Twitchell AM, Hogan JE, Aulton ME. Assessment of thickness variation and surface-roughness of aqueous film-coated tablets using a light-section microscope. *Drug Dev Ind Pharm*. 1995;21:1611–1619.
11. Ruotsalainen M, Heinamaki J, Guo HX, Laitinen N, Yliruusi J. A novel technique for imaging film coating defects in the film-core interface and surface of coated tablets. *Eur J Pharm Biopharm*. 2003;56:381–388.
12. Tobiska S, Kleinebudde P. Coating uniformity: influence of atomizing air pressure. *Pharm Dev Technol*. 2003;8:39–46.
13. Rege BD, Gawel J, Kou JH. Identification of critical process variables for coating actives onto tablets via statistically designed experiments. *Int J Pharm*. 2002;237:87–94.
14. Porter SC, Verseput RP, Cunningham CR. Process optimization using design of experiments. *Pharm Technol*. 1997;21:1–7.
15. Mowery MD, Sing R, Kirsch J, Razaghi A, Bechard S, Reed RA. Rapid at-line analysis of coating thickness and uniformity on tablets using laser induced breakdown spectroscopy. *J Pharm Biomed Anal*. 2002;28:935–943.
16. Aulton ME. *Surface effects in film coating*. In: Cole GC, Hogan JE, Aulton ME, editors. *Pharmaceutical Coating Technology*. Bristol, PA: Taylor & Francis, 1995.
17. Aulton ME. *Mechanical properties of film coats*. In: Cole GC; Hogan JE, Aulton ME, editors. *Pharmaceutical Coating Technology*. Bristol, PA: Taylor & Francis, 1995.
18. Scattergood LK, Cunningham CR, Vesey CF, Fegely KA. Optimization of spray-nozzle performance for aqueous film coating processes. Presented at the 3rd World Meeting APV/APGI, Berlin, 3-6 April, 2000.
19. Toschkoff G, Suzzi D, Tritthart W, Reiter F, Schlingmann M, Khinast JG. Detailed analysis of air flow and spray loss in a pharmaceutical coating process. *AIChE J*. In press.
20. Durst F, Tropea C. The slit effect in phase Doppler anemometry. *Mod Techniques Meas Fluid Flows*. The 2nd International Conference on Fluid Dynamic Measurement and Its Applications (IFCDMA), Tsinghua Univ, Beijing, China; 19-22 Oct. 1994. pp. 38–43.
21. Xu TH, Tropea C. Improving the performance of 2-component phase Doppler anemometers. *Meas Sci Technol*. 1994;5:969–975.
22. Tropea C, Xu TH, Onofri F, Grehan G, Haugen P, Stieglmeier M. Dual-mode phase-Doppler anemometer. *Part Part Syst Charact*. 1996;13:165–170.
23. Dullenkopf K, Willmann M, Wittig S, Schone F, Stieglmeier M, Tropea C, Mundo C. Comparative mass flux measurements in sprays using a patternator and the phase-Doppler technique. *Part Part Syst Charact*. 1998;15:81–89.
24. Roisman IV, Tropea C. Flux measurements in sprays using phase Doppler techniques. *Atom Sprays*. 2001;11:667–699.
25. McDonnell VG, Cameron CD, Samuelsen GS. Symmetry assessment of an air-blast atomizer spray. *J Propul Power*. 1990;6:375–381.
26. Lazaro BJ. *Evaluation of Phase Doppler Particle Sizing in the Measurement of Optically Thick, High Number Density Sprays*. East Hartford, CT: United Technologies Research Center, 1991.UTRC91–11.
27. VandenMoortel T, Santini R, Tadrist L, Pantaloni J. Experimental study of the particle flow in a circulating fluidized bed using a phase Doppler particle analyser: a new post-processing data algorithm. *Int J Multiphase Flow*. 1997;23:1189–1209.
28. Widmann JF, Presser C, Leigh SD. Identifying burst splitting events in phase Doppler interferometry measurements. *Atom Sprays*. 2001;11:711–733.
29. Widmann JF, Presser C, Leigh SD. Improving phase Doppler volume flux measurements in low data rate applications. *Meas Sci Technol*. 2001;12:1180–1190.
30. Chao J, Hwang K, Lee T. Sensitivity of user parameter settings of phase Doppler analyzer in combusting spray. Presented at the AIAA 21st Fluid Dynamics, Plasma Dynamics and Laser Conference, Seattle, WA, June 18–20, 1990.
31. Kapulla R, Najera SB. Operation conditions of a phase Doppler anemometer: droplet size measurements with laser beam power, photomultiplier voltage, signal gain and signal-to-noise ratio as parameters. *Meas Sci Technol*. 2006;17:221–227.

32. Friedman JA, Renksizbulut M. A method for increasing the sensitivity of phase Doppler interferometry to seed particles in liquid spray flows. *Part Part Syst Charact*. 1995;12:225–231.
33. Widmann JF, Presser C, Leigh SD. Extending the dynamic range of phase Doppler interferometry measurements. *Atom Sprays*. 2002;12:513–537.
34. Sankar SV, Inenaga A, Bachalo WD. Trajectory dependent scattering in phase Doppler interferometry: minimizing and eliminating sizing error. Presented at the 6th International Symposium of Application of Laser Techniques to Fluid Mechanics, 20-23 July 1992 and Lisbon, Portugal, 1992.
35. Muliadi AR, Sojka PE, Sivathanu Y, Lim J. A comparison of phase Doppler analyzer (dual-PDA) and optical patternator data for twin-fluid and pressure-swirl atomizer sprays. *ASME J Fluids Eng*. 2010;32:0614021–06140210.
36. Aulton ME, Twitchell AM. *Solution properties and atomization in film coating*. In: Cole G, editor. *Pharmaceutical Coating Technology*. Bristol, PA: Taylor & Francis; 1995.
37. Muller R, Kleinebudde P. Comparison study of laboratory and production spray guns in film coating: effect of pattern air and nozzle diameter. *Pharm Dev Technol*. 2006;11:425–433.
38. Varga CM, Lasheras JC, Hopfinger EJ. Initial breakup of a small-diameter liquid jet by a high-speed gas stream. *J Fluid Mech*. 2003;497:405–434.
39. Gretzinger J, Marshall WR. Characteristics of pneumatic atomization. *AIChE J*. 1961;7:312–318.
40. Kim KY, Marshall WR. Drop-size distributions from pneumatic atomizers. *AIChE J*. 1971;17:575–584.
41. Cohen RD. Effect of viscosity on drop breakup. *Int J Multiphase Flow*. 1994;20:211–216.
42. Lefebvre AH. *Atomization and Sprays*. Levittown, PA: Taylor & Francis, 1989.

Manuscript received Feb. 17, 2011, and revision received Aug. 2, 2011.